JOURNAL OF APPLIED ELECTROCHEMISTRY 21 (1991) 1058–1062

Inertial characteristics of velocity and shear stress electrochemical probes*

P. I. GESHEV

Thermophysics Institute, Lavrent'ev, Str. 1, Novosibirsk, 630090, USSR

Received 1 February 1991; revised 25 April 1991

Numerically obtained frequency response functions for various electrochemical velocity and shear stress probes used in hydrodynamical measurements are presented.

1. Introduction

The inertia of electrochemical probes is due to the ionic convective diffusion processes to or from the electrode surface. For estimation and correction of this inertia it is necessary to calculate the frequency response function (FRF) of the probe. FRF is the ratio of two complex amplitudes, output amplitude to input amplitude. This characteristic may be introduced only for linear systems. Therefore the governing equations were linearized for the calculation of FRF. The linearization is valid provided all fluctuations are small compared to their mean values. The FRF was calculated for spherical, cylindrical, 'tip point' velocity probes and also for rectangular, circular and split circular shear stress sensors. The results of calculation for the FRF are given in the form of approximate formulae. The FRF expressions may be used to correct probe signals.

2. Inertia of the velocity probes

If the turbulence intensity is not very high the operation of electrochemical velocity and shear stress probes can be described by linearized equations of convective diffusion

$$(\boldsymbol{u} \cdot \nabla)c = D \frac{\partial^2 c}{\partial y^2} \tag{1}$$

$$\frac{\partial c'}{\partial t} + (\boldsymbol{u} \cdot \nabla)c' + (\boldsymbol{u}' \cdot \nabla)c = D \frac{\partial^2 c'}{\partial y^2} \tag{2}$$

where D is the diffusion coefficient, c, c', $\boldsymbol{u}$, $\boldsymbol{u}'$ are the average and fluctuating concentrations of control ions and velocities, respectively, y is the coordinate normal to the electrode surface.

Inertial properties of linear systems are described by the so called complex frequency response function (FRF), which is determined by the ratio of two complex amplitudes of output and input signals

$$H(\omega) = \frac{A_{\text{out}}(\omega)}{A_{\text{in}}(\omega)} \tag{3}$$

Here a dimensionless normalized FRF determined by the formula

$$\bar{H}(\omega) = \frac{H(\omega)}{H(0)} = \frac{A_{\text{out}}(\omega)}{A_{\text{out}}(0)} \frac{A_{\text{in}}(0)}{A_{\text{in}}(\omega)} \tag{4}$$

is used.

The modulus of the function $\bar{H}(\omega)$ shows damping of the signals due to viscosity and diffusivity effects. The argument of the function $\bar{H}(\omega)$ gives the phase lag between output and input signals. For velocity probes the input signal is, of course, the fluctuation of liquid velocity in the vicinity of the probe, $\tilde{U}$. For shear stress probes the input signal is the wall shear stress fluctuation, $\tilde{\tau}$. The output signal is always the fluctuation of the diffusion current, $\tilde{I}$.

Velocity fields around a sphere and a cylinder in a flow with imposed oscillations were calculated by Illingworth [3] for small Reynolds number (the Stokes approach). Fluctuating currents for a sphere and a cylinder were calculated in [1, 2] at large Peclet number in a boundary layer approach. It is convenient to present the FRF for velocity probes as a product of two multipliers, the hydrodynamic and diffusion parts of FRF

$$H_{\text{h}}(\omega) = \frac{\tilde{\tau}(\omega)}{\tilde{U}_\infty(\omega)}, \qquad H_{\text{d}}(\omega) = \frac{\tilde{I}(\omega)}{\tilde{\tau}(\omega)} \tag{5}$$

where $\tilde{\tau}(\omega)$ is the shear stress fluctuation averaged over the probe surface.

The hydrodynamic part of the FRF can be obtained from Illingworth [3]:

(a) for a sphere

$$\bar{H}_{\text{h}} = 1 + \frac{Re}{8}\left(\frac{1 + 8i\bar{\omega} - (1 + 4i\bar{\omega})^{1/2}}{1 + (1 + 4i\bar{\omega})^{1/2}}\right) \tag{6}$$

(b) for a cylinder

$$\bar{H}_{\text{h}}^{\text{cyl}} = \left[1 + \frac{4i\bar{\omega} - (1 + 4i\bar{\omega}) \ln (1 + 4i\bar{\omega})}{8i\bar{\omega}(1 - \ln Re)}\right]^{-1} \tag{7}$$

where $\bar{\omega} = \omega\nu/U_\infty^2$, $Re = U_\infty d/\nu \ll 1$, d is the probe diameter, U_∞ is the mean flow velocity, ν is liquid viscosity. According to [3] Equations 6 and 7 are valid for the frequency domain $\bar{\omega}Re < 1$.

An approximate formula for the diffusion part of

* This paper was presented at the Workshop on Electrodiffusion Flow Diagnostics, CHISA, Prague, August 1990.

0021-891X/91 $03.00 + .12

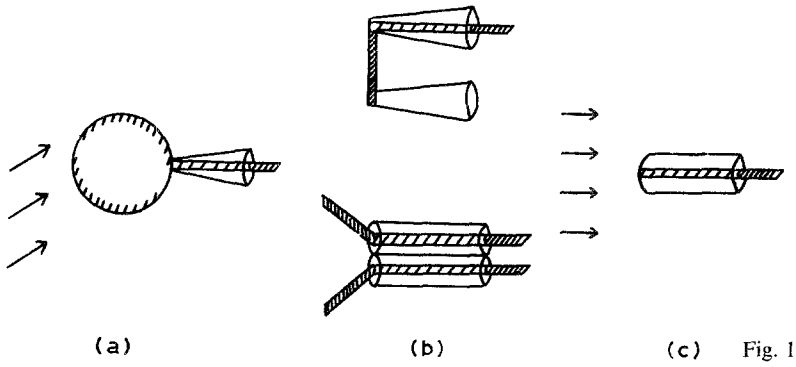

Fig. 1. Various shapes of velocity probes.

the FRF for a sphere was obtained in [1]

$$|\bar{H}_d| = \left(\frac{1 + 1.9 \times 10^{-3}\sigma^2}{1 + 1.3 \times 10^{-2}\sigma^2 + 3.5 \times 10^{-5}\sigma^4}\right)^{3/4} \quad (8)$$

$$\arg(\bar{H}_d) = -1.5 \arctan[0.117 \times \sigma(1 + 7.5 \times 10^{-4}\sigma^2)] \quad (9)$$

where $\sigma = (\omega/D)[Dd^2/U_\infty A_0]^{2/3}$, $A_0 = 1 + 3Re/16$.

It was found in [1] that the diffusion part of the FRF for a cylinder can be expressed through the spherical FRF $\bar{H}_d$ by the formula

$$\bar{H}_d^{cyl}(\sigma') = \bar{H}_d(1.16\sigma') \quad (10)$$

where $\sigma' = (\omega/D)[Dd^2/U_\infty B_0]^{2/3}$, $B_0 = (2 - \ln Re)^{-1}$.

Expressions 8–10 are valid for all σ and σ'.

Spectral amplitudes of fluctuating flow velocities $\tilde{U}_\infty(\omega)$ and currents $\tilde{I}(\omega)$ are connected by formulae [1]

(a) for a sphere

$$\frac{\tilde{I}(\omega)}{I_0} = \frac{\tilde{U}_\infty(\omega)}{3U_\infty}\left(1 + \frac{3Re}{16}\right)\bar{H}_h(\bar{\omega})\bar{H}_d(\sigma) \quad (11)$$

(b) for a cylinder

$$\frac{\tilde{I}(\omega)}{I_0} = \frac{\tilde{U}_\infty(\omega)}{3U_\infty}\left(1 + \frac{1}{1 - \ln Re}\right)\bar{H}_h^{cyl}(\bar{\omega})\bar{H}_d^{cyl}(\sigma') \quad (12)$$

where I_0 is the average probe current.

Another approach (the boundary layer approach) which is valid at $Re \gg 1$ was used for the calculation of the hydrodynamic part of FRF for the so called 'tip point' velocity probe [1] (Fig. 1c). The approximations for the FRF of this probe are

$$|\bar{H}_h| = (1 + \omega_+^2/15)^{1/4} \quad (13)$$

$$\arg(\bar{H}_h) = 0.5 \arctan(0.256\,\omega_+) \quad (14)$$

$$|\bar{H}_d| = \left(\frac{1 + 2.32 \times 10^{-3}\omega_-^2}{1 + 4.45 \times 10^{-2}\omega_-^2 + 1.49 \times 10^{-4}\omega_-^4}\right)^{3/4} \quad (15)$$

$$\arg(\bar{H}_d) = -1.5 \arctan[0.211 \times \omega_-(1 + 2.04 \times 10^{-3}\omega_-^2)] \quad (16)$$

where $\omega_+ = (\omega/a_0)$, $\omega_- = (\omega/a_0)[\nu/D]^{1/3}$, $a_0 = kU_\infty/d$, k is a probe shape constant ($2 < k < 4$) obtained in [1] from the potential flow solution. The FRF of the 'tip point' velocity probe is shown on Fig. 3.

3. Inertia of the shear stress probes

For shear stress probes only the diffusion FRF needs to be calculated [1, 2, 4]. New variables can be introduced

$$\eta = y\left(\frac{\tau_0}{(x - x_1)\mu D}\right)^{1/3}, \quad \xi = \omega\left(\frac{\mu^2(x - x_1)^2}{D\tau_0^2}\right)^{1/3},$$

$$h = \frac{c'}{c_\infty}\left(\frac{\tilde{\tau}_x}{\tau_0} - \frac{dx_1}{dz}\frac{\tilde{\tau}_z}{\tau_0}\right)^{-1} \quad (17)$$

where $\mu = \rho\nu$ is the viscosity of the liquid, $(x - x_1)$

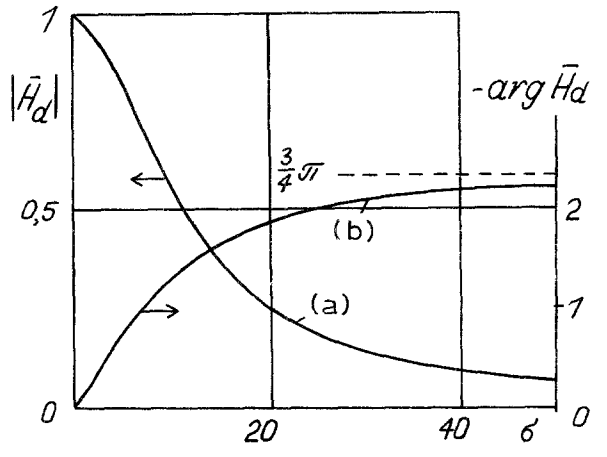

Fig. 2. FRF for spherical velocity probes: (a) modulus of FRF, (b) argument of FRF.

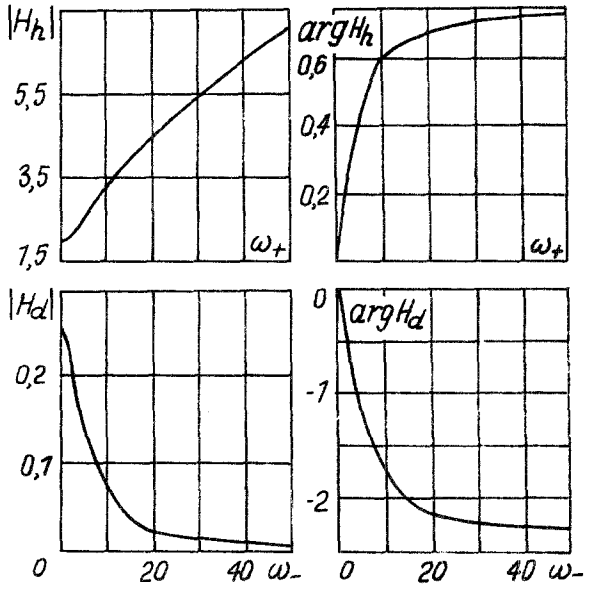

Fig. 3. FRF for "tip nose" velocity probes: (H_h) hydrodynamic FRF, (H_d) diffusion FRF.

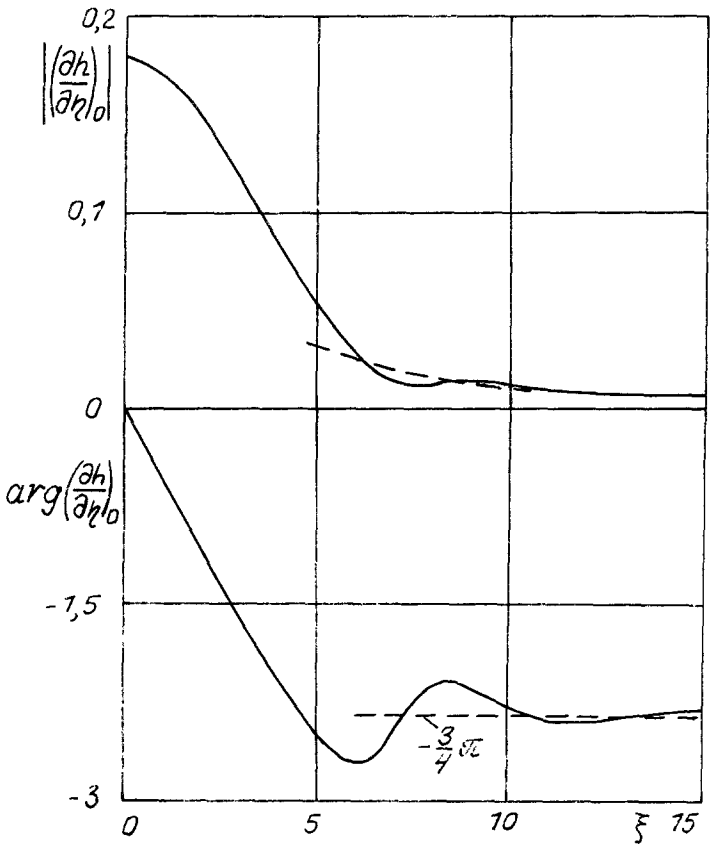

Fig. 4. Modified density of the fluctuating mass flux $j' = (dh/d\eta)_0$: (a) modulus j', (b) argument j'.

is the distance from the upper boundary of the probe electrode, τ_0 is the mean shear stress on the probe, $\tilde{\tau}_{x,z}(\omega)$ is the fluctuation amplitude of the two components of the shear stress vector. The modified density of the fluctuating mass flux $j' = (\partial h/\partial\eta)_{\eta=0}$ was calculated using the boundary layer approach (Fig. 4 shows amplitude and phase lag of j'). Further integration of j' over probe surfaces of various shapes produced a FRF for

(a) a rectangular electrode (Fig. 5a)

$$H(\sigma) = \frac{3}{2\sigma}\int_0^\sigma j'(\xi)\mathrm{d}\xi \tag{18}$$

(b) a circular electrode (Fig. 5c)

$$H_x(\sigma) = \frac{3}{2\sigma^{5/2}}\int_0^\sigma (\sigma^3 - \xi^3)^{1/2} j'(\xi)\mathrm{d}\xi \tag{19}$$

(c) a differential electrode composed of two halves of a disc (Fig. 5c)

$$H_z(\sigma) = \frac{3}{2\sigma^{5/2}}\int_0^\sigma (\sigma^{3/2} - \xi^{3/2})\, j'(\xi)\mathrm{d}\xi \tag{20}$$

where $\sigma = \omega T$ is a dimensionless frequency, T is a characteristic time constant determined below. Normalized FRF were calculated from Equations 18–20.

Results are shown in Fig. 6 and can be summarized by the approximate formulae expressed in Equations 21–28:

(a) for $\sigma < 6$

$$|\bar{H}_x| = (1 + 0.049\,\sigma^2 + 0.0006\,\sigma^4)^{-1/2} \tag{21}$$

$$|\bar{H}| = (1 + 0.056\,\sigma^2 + 0.00126\,\sigma^4)^{-1/2} \tag{22}$$

$$\arg(\bar{H}_x) = -\arctan[0.242\,\sigma(1 + 0.0124\,\sigma^2 - 0.00015\,\sigma^4)] \tag{23}$$

$$\mathrm{rg}(\bar{H}) = -\arctan[0.276\,\sigma(1 + 0.02\,\sigma^2 - 0.00026\,\sigma^4)] \tag{24}$$

(b) for $\sigma \geqslant 6$

$$|\bar{H}_x| = \frac{4.4}{\sigma}\left[1 - \frac{1.7}{(\sigma)^{1/2}} + \frac{1.3}{\sigma}\right]^{1/2} \tag{25}$$

$$|\bar{H}| = \frac{3.7}{\sigma}\left[1 - \frac{1.5}{(\sigma)^{1/2}} + \frac{1.1}{\sigma}\right]^{1/2} \tag{26}$$

$$\arg(\bar{H}_x) = -\arctan(1.16(\sigma)^{1/2} - 1) \tag{27}$$

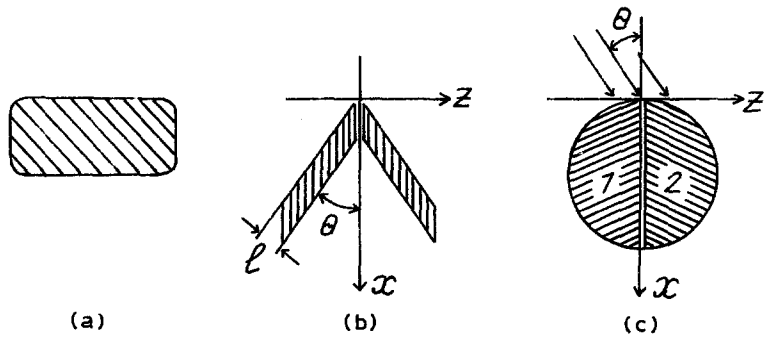

Fig. 5. Various types of shear stress probes: (a) rectangular, (b) Λ-shape, (c) split circular electrode.

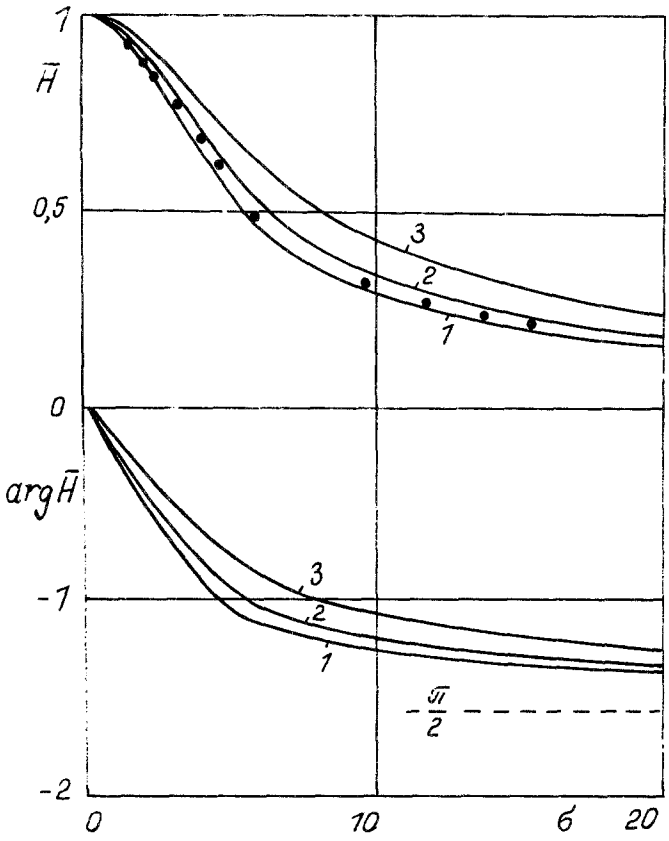

Fig. 6. Modulus and argument of FRF for shear stress probes: (1) rectangular, (2) circular electrode, (3) circular z-pulsation probe, (●) FRF from Hanratty & Chorn [5].

$$\arg(\bar{H}) = -\arctan(1.32(\sigma)^{1/2} - 1). \quad (28)$$

All the approximate formulae have a deviation from the calculated value of not more than 1%.

Convenient formulae can be obtained for correction of probe signals for the three shapes shown in Fig. 5. These are

$$\frac{\tilde{\tau}_x(\omega)}{\tau_0} = 3\frac{\tilde{I}(\omega)}{I_0\bar{H}(\omega T'')} \quad \text{(Fig. 5a)} \quad (29)$$

$$\frac{\tilde{\tau}_{x,z}(\omega)}{\tau_0} = 3\frac{\tilde{I}_1(\omega) \pm \tilde{I}_2(\omega)}{I_0\bar{H}(\omega T')} \quad \text{(Fig. 5b)} \quad (30)$$

$$\frac{\tilde{\tau}_x(\omega)}{\tau_0} = 3.82\frac{\tilde{I}_1(\omega) + \tilde{I}_2(\omega)}{I_0\bar{H}_x(\omega T)} \quad \text{(Fig. 5c)} \quad (31)$$

$$\frac{\tilde{\tau}_z(\omega)}{\tau_0} = 5.36\frac{\tilde{I}_1(\omega) - \tilde{I}_2(\omega)}{I_0\bar{H}_z(\omega T)} \quad \text{(Fig. 5c)} \quad (32)$$

where I_0 is the average probe current, $\tilde{I}_{1,2}(\omega)$, $\tilde{I}(\omega)$ are the fluctuation amplitudes of currents from different parts of the probe. Characteristic time constants of the probes from Equations 29–32 are

$$T = \left(\frac{\mu^2 d^2}{D\tau_0^2}\right)^{1/3} \qquad T' = \left(\frac{\mu^2 l^2}{D\tau_0^2 \sin^2\theta}\right)^{1/3}$$

$$T'' = \left(\frac{\mu^2 l^2}{D\tau_0^2}\right)^{1/3} \quad (33)$$

where 2θ is the angle between two thin strip electrodes (Fig. 5b). There is a possibility of determining the time constants in Equation 33 from non-stationary currents which occur in switch processes of electrodes when a step change in electrochemical potential is applied. The curves shown in Fig. 7 were calculated in [1] (and also [7]) by using analytical expressions for local mass flux density, $j(x, t)$, extracted from the solution of the transient Leveque problem given in [6]. Curve 1 shows the dependence of the ratio $j(x, t)/j(x, \infty)$ on non-dimensional time $\bar{t} = t(\mu^2(x - x_1)^2/(D\tau_0^2))^{-1/3}$. The relative current for the probe of rectangular shape is shown by curve 2, Fig. 7, and is given by formula

$$\frac{I(t)}{I(\infty)} = \left\{1 - \exp\left[-3.3\left(\frac{t}{T''}\right)^{5/3}\right]\right\}^{-0.3} \quad (34)$$

and for the circular electrode (curve 3, Fig. 7) by the expression

$$\frac{I(t)}{I(\infty)} = \left\{1 - \exp\left[-4\left(\frac{t}{T}\right)^{5/3}\right]\right\}^{-0.3} \quad (35)$$

There is no need to determine separately values of D, τ_0, μ, l and d, which characterize the time constants T, T', T'' of the probes, because these constants can be

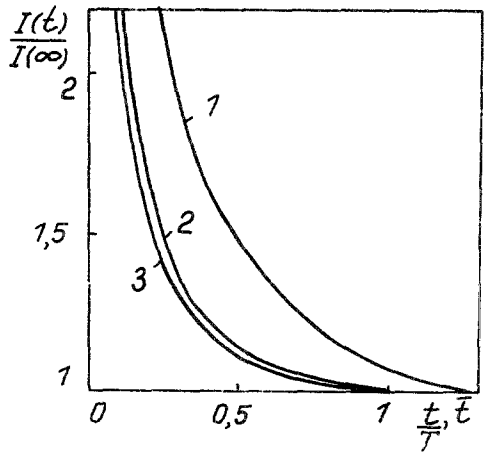

Fig. 7. Transient currents in switching process: (1) for density of mass flux, (2) for rectangular, (3) for circular electrode.

easily determined from Equations 34 and 35 for the transient process.

If the FRF is used to correct the signal the frequency range of probe operation may be expanded by a factor of 10. The expressions represented by Equations 29–32 are, of course, for spectral measurements. But if the FRF of the probe is known, a numerical algorithm for correction of real (on line) signals can be constructed.

References

[1] V. E. Nakoryakov, A. P. Burdukov, O. N. Kashinsky and P. I. Geshev, 'Electrodiffusion method of investigation into local structure of turbulent flows', Thermophysics Institute Novosibirsk (1986). 247 p. (in Russian).

[2] Y. E. Bogolyubov, P. I. Geshev, V. E. Nakoryakov and I. A. Ogorodnikov, *J. Appl. Mech. Tech. Phys.* **13** (1972) N 14.

[3] C. R. Illingworth, *Z. Angew. Math. Phys.* **14** (1963) 681.

[4] G. Fortuna and T. J. Hanratty, *Int. J. Heat Mass Transfer* **14** (1971) 1499.

[5] T. J. Hanratty and L. G. Chorn, 'Turbulence in liquids', Symposium on Turbulence, 1975, Science Press, Princeton, NJ (1977) p. 244.

[6] M. Soliman and P. L. Chambre, *Int. J. Heat Mass Transfer* **10** (1967) 169.

[7] O. Wein, *Collect. Czech. Chem. Commun.* **46** (1981) 3209.